

Model-Based Relevance of Measuring Electrodes for the Inverse Solution with a Single Dipole

Beata Ondrusova^{1,2}, Jana Svehlikova¹, Jan Zelinka¹, Milan Tysler¹, Peter Tino³

¹Institute of Measurement Science, Slovak Academy of Sciences, Bratislava, Slovakia

²Faculty of Electrical Engineering and Information, Slovak University of Technology, Bratislava, Slovakia

³School of Computer Science, University of Birmingham, Birmingham, United Kingdom

Abstract

Individual ECG electrodes of a multi-lead measuring system can have a variable impact on the solution of the inverse problem. In this study, we investigated the model-based relevance of individual ECG electrodes to identify the position of the stimulation electrode using the inverse solution with a single dipole as an equivalent electrical heart generator. We used four torso ECG mapping datasets from the EDGAR database recorded during ventricular stimulation in three animal torso-tank experiments and one human measurement. The relevance of electrodes, expressed as their weighted contributions to the inverse solution, was determined by the singular value decomposition of a transfer matrix calculated for the given position of the stimulation electrode. The results showed that gradual omission of the electrodes with the highest weighted contributions to the inverse solution worsens the localization. However, missing a small number of such electrodes has little or no effect on the localization. One dataset was more robust to the gradual omission of electrodes with the highest contributions, and the localization significantly deteriorated only after skipping 92% of electrodes. Further study showed that using only several electrodes with the highest weighted contributions to the inverse solution leads to the same or even better localization results than using all electrodes.

1. Introduction

The solution of the inverse problem of electrocardiography, also called electrocardiographic imaging, provides information about the heart activity from measured electrical potentials on the torso obtained by a multi-lead ECG measuring system and from the geometrical model of the torso constructed from the CT/MRI scans [1]. The solution is also used to noninvasively identify the origin of the atria arrhythmias such as the focal atrial tachycardia [2] or ventricular arrhythmias such as the premature ventricular contractions

(PVCs) [3].

The multi-lead ECG measuring system uses many electrodes distributed on the torso to record the surface electrical potentials. There is no golden standard for the number of electrodes used and the positions of electrodes on the torso for the accurate solution of the inverse problem. Therefore, the current research is focused on determining the number and positions of electrodes needed to solve the inverse problem accurately. Some studies show that good localization results can be obtained also with a reduced number of electrodes for the solution of the inverse problem [4], [5].

In this study, we examine how individual electrodes affect the localization of the stimulation electrode by the inverse solution with a single dipole model of the cardiac electric generator based on their relevance derived from a transfer matrix.

2. Materials and Methods

The workflow of this study is depicted in Figure 1. The individual steps of this study are described in more detail in the following paragraphs.

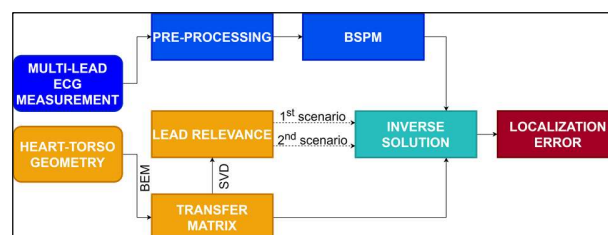


Figure 1. The workflow of the study.

Data: This study explores four torso ECG mapping datasets from three animal torso-tank experiments and one measurement on patient obtained from the EDGAR database [6]. Each dataset contains signals recorded by the multi-lead ECG measuring system during the ventricular stimulation and the heart-torso geometry. The Utah tank 1 and Utah tank 2 datasets were provided by the Scientific Computing and Imaging Institute in Salt Lake City, Utah.

The Bordeaux tank dataset was provided by the Liryc-the Electrophysiology and Heart Modelling Institute in Bordeaux, France. The Bratislava human dataset was obtained by the Institute of Measurement Science in cooperation with the National Institute for Cardiovascular Diseases in Bratislava, Slovakia. More detailed information about datasets is shown in Table 1 and can be found at www.ecg-imaging.org/edgar-database.

Table 1. Information about used datasets.

Dataset	Type	Torso electrodes	Sampling frequency	Transfer matrix size
Utah tank 1	Canine model	192	1 kHz	192 x 741
Utah tank 2	Canine model	192	1 kHz	192 x 1011
Bordeaux tank	Porcine model	128	2 kHz	128 x 2682
Bratislava human	Patient with pacemaker	128	1 kHz	128 x 4584

Pre-processing: All body surface recordings were analyzed to identify electrodes with insufficient ECG signal quality. The cubic spline interpolation was used to remove baseline wandering in measured ECG signals. The ECG beats were segmented from measured ECG signals based on predefined time intervals around the R-peak. The ECG beats were aligned with respect to the R-peak and then clustered according to their morphology by employing the *k means* algorithm. Subsequently, the ECG beats within the cluster were averaged to improve the signal to noise ratio. For each dataset, the body surface potential maps (BSPMs) were computed in each time instant for the averaged ECG beat.

Lead relevance: The transfer matrix was calculated using a model-specific homogeneous torso geometry employing the Boundary Element Method (BEM) for each dataset. If we consider a single dipole as an equivalent heart generator, then the transfer matrix size is $m \times 3 * n$, where m is the number of electrodes on the body surface and n is the number of heart dipoles with three orthogonal components. If Φ is the known electrical potential vector measured on the torso surface, T^+ is a pseudoinverse of the transfer matrix, then (assuming T is full rank) the inverse problem estimates unknown electrical heart generator H using the equation

$$H = T^+ \Phi. \quad (1)$$

The singular value decomposition (SVD) of the transfer matrix was used to determine the contributions of the individual torso electrodes to the solution of the inverse problem. We examine the position corresponding to the true initial site of the heart activation to determine the contributions of individual electrodes to the solution of the inverse problem. Therefore, let A be an $m \times 3$ submatrix

of the whole transfer matrix T corresponding to a specific position of a single dipole (tip of the stimulation electrode). The pseudoinverse of the transfer matrix A^+ is expressed as

$$A^+ = V \Sigma^{-1} U^T, \quad (2)$$

where matrices V and U are orthogonal and matrix Σ^{-1} is a diagonal matrix with reciprocals of the singular values on the diagonal and zeros in all off-diagonal entries. The weighted contribution v of a torso electrode k ($1 \leq k \leq m$) to the inverse solution is expressed as

$$v_k = \sum_{i=1}^3 \frac{1}{\sigma_i} |u_{ki}|, \quad (3)$$

where σ_i is the i th entry on a diagonal of the matrix Σ and u_{ki} is the k th entry of the i th column vector of U [7].

Inverse solution: The inverse problem of electrocardiography was used to estimate the location of the initial site of the heart activation that corresponds to the position of the stimulation electrode. A single dipole was assumed as an equivalent electric generator. The best position of electrical generator H is searched through the predefined positions within the heart epicardium and must satisfy the criterion of the minimal relative residual error (RRE) within the time interval from the very beginning of depolarization up to 25 ms. The RRE is calculated for every possible position of an electric generator H in the time instant as

$$RRE = \frac{\sqrt{\sum_{i=1}^m (\Phi_{M_i} - \Phi_{C_i})^2}}{\sqrt{\sum_{i=1}^m \Phi_{M_i}^2}}, \quad (4)$$

where Φ_M is the measured map and Φ_C is the map computed from a dipole estimated by the inverse solution.

In this study, we investigated two scenarios:

The first scenario - we gradually removed the electrodes from the inverse solution, starting with the one which has the highest weighted contribution to the inverse solution. In the end, we ended up only with the 3 electrodes with the lowest weighted contributions for the inverse solution.

The second scenario - we started to solve the inverse problem using the 3 electrodes with the highest weighted contributions, and then we gradually added more electrodes until we used the full data set.

For all solutions, the localization error (LE) was calculated using the following formula:

$$LE = \sqrt{\sum_{i=1}^3 (x_{T_i} - x_{R_i})^2}, \quad (5)$$

where x_T are cartesian coordinates of the known position of the stimulation electrode (true position) and x_R are cartesian coordinates of the position calculated by the inverse solution.

3. Results

The SVD of a submatrix of the transfer matrix corresponding to a single dipole placed at the tip of the stimulation electrode was examined to determine the weighted contributions of individual electrodes to the inverse solution. The weighted contributions of electrodes to the inverse solutions for all datasets are depicted in Figure 2. The electrodes with the highest contributions are shown in the red color scale, while those with the smallest contributions are in the blue color scale. The electrodes with the highest contributions are located on the torso surface close to the position of the stimulation electrode.

In the first scenario, we analyzed how removing electrodes with the highest weighted contributions affects the inverse localization. For the Utah tank 1, the LE started to increase from 18.0 mm after removing 36 (19%) electrodes with the highest contributions and continued to increase up to 55.7 mm with further electrode removal. For the Utah tank 2, we observed robustness to electrode removal. The LE did not increase until 177 (92%) of electrodes were removed. For the Bordeaux tank, the LE gradually increased from 12.5 mm after removing 12 (9%) to 62.9 mm. For the Bratislava human data, the LE increased from 16.0 mm after removing just 6 (5%) electrodes and worsened rapidly after removing 24 (19%) electrodes to 121.2 mm. From Figure 2 it can be seen that the LE decreased with the specific number of omitted electrodes, mainly in the case of the Bordeaux tank and Bratislava human. To explain this improvement in the LE, the RRE distribution on the heart epicardium was inspected. In Figure 3, we can see the RRE distribution on epicardium for the Bratislava human data. The area on epicardium in which we find small values of RRE on epicardium becomes larger with the increasing number of omitted electrodes. Therefore, the identification of minimal RRE on epicardium becomes ambiguous.

Further, we implemented the second scenario and investigated the LE of the inverse solution obtained using the 3 electrodes with the highest weighted contributions up to the full number of electrodes (full set). For the Utah tank 1, the LE started to decrease from 54.5 mm obtained using the 3 (2%) electrodes with the highest weighted contributions to 4.2 mm. The decrease of the LE was followed by a gradual increase up to the LE calculated for the full set. For the Utah tank 2, the worst LE equaled to 57.2 mm and was obtained when 12 (6%) electrodes with the highest weighted contributions for the inverse solution were used. After that, the LE was stable and equaled to the LE obtained by using the full set. For the Bordeaux tank, the LE started to decrease from 62.0 mm when only 3 (2%) electrodes with the highest weighted contributions were used up to 9.0 mm. After the initial decrease, the LE was stable. For the Bratislava human, the worst LE equaled to 114.8 mm and was obtained when 5 (4%) electrodes with the highest weighted contributions were used. The

decrease of the LE was followed by a gradual increase up to the LE for the full set. Table 2 contains the summary of results for both scenarios. The minimal and maximal theoretical LE is calculated as the distance between the known true position of the stimulation electrode and the nearest and furthest mesh point. The calculated LE is computed using Equation 5.

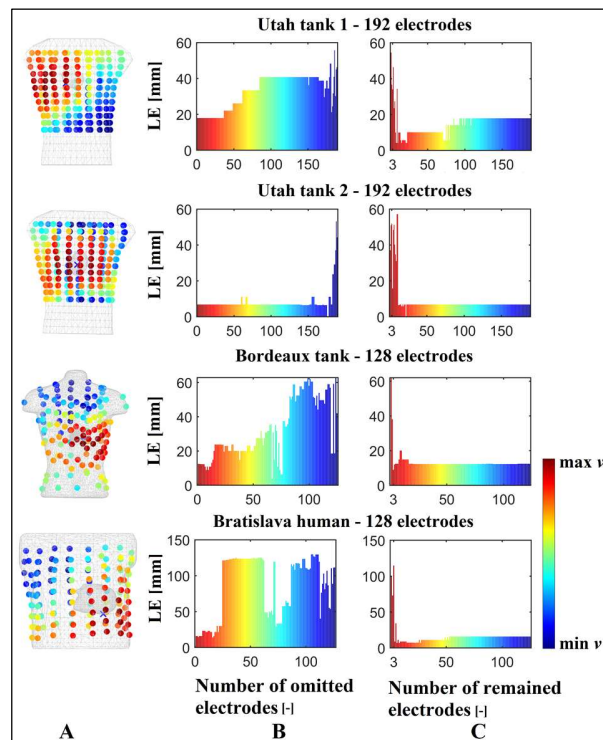


Figure 2. A) The weighted contributions of torso electrodes (the position of the stimulation electrode – blue cross), B) The LE for the 1st scenario, C) The LE for the 2nd scenario.

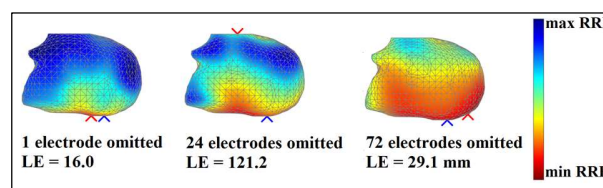


Figure 3. The RRE distribution on epicardium for the Bratislava human (the position of the stimulation electrode – blue cross, the position of min RRE – red cross).

Table 2. The theoretical and calculated LE in mm.

Dataset	Full set	Theoretical		Calculated			
		Min	Max	1 st scenario		2 nd scenario	
Utah tank 1	18.0	4.2	62.0	18.0	55.7	4.2	54.5
Utah tank 2	6.9	0.0	60.3	0.0	53.2	0.0	57.2
Bordeaux tank	12.5	1.5	79.5	3.9	62.9	9.0	62.0
Bratislava human	16.0	1.6	134.1	14.1	129.8	7.1	114.8

4. Discussion

In this study, we investigated the model-based relevance of the torso electrodes in terms of their contributions to the solution of the inverse problem. The weighted contributions for four well-defined datasets were calculated from the transfer matrix by using the SVD. The positions of torso electrodes with the highest contributions reflect the position of the stimulation electrode placed in the ventricle. Therefore, if the origin of the heart activity is located posteriorly, the electrodes with the highest contributions for the solution of the inverse problem can be located on the back.

Next, we implemented two scenarios. The first one is the worst-case scenario when we omitted the torso electrodes with the highest contributions to the solution of the inverse problem for the true position of the origin of the heart activity. The results showed that the Utah tank 2 dataset is more robust, and with the increasing number of the omitted electrodes, the LE does not change. In contrast, the datasets Utah tank 1, Bordeaux tank and Bratislava human are more sensitive to the omitted electrodes with the highest contributions. A rapid increase of the LE was observed for the Bratislava human dataset after omitting 24 electrodes with the highest contributions. This result could be explained by the fact that the homogeneous computational model represents truly experiments in the homogeneous tank while the Bratislava human data are more complex, and the computational model is only its approximation and therefore is more sensitive to the missing information from the most significant electrodes.

In the second scenario, we investigated the LE obtained using a limited number of electrodes with the highest contributions to the inverse solution. The results showed that we can obtain a good localization even if we do not use the full set of electrodes. Moreover, the LE obtained when using the limited number of electrodes with the highest contributions can be smaller compared to the LE obtained by using the full set of electrodes, as in the case of the Utah tank 1 and Bratislava human datasets. This can result from the fact that signals measured by the electrodes with the highest contributions to the solution of the inverse problem carry the most important information for the solution, while the information from other electrodes can bring uncertainties to the solution of the inverse problem.

5. Conclusions

The model-based relevance of measuring electrodes expressed as their weighted contributions to the inverse solution was derived by the SVD of a transfer matrix. The study showed that omitting a few electrodes with the highest weighted relevance from the inverse solution with a single dipole as an equivalent heart generator does not severely impact the localization. The results indicate that

the same or better localization can be obtained by using a limited number of electrodes with the highest relevance instead of using a full set of electrodes. However, this study was performed using well-defined datasets, meaning that the origin of the heart activity was known. We do not have this information for real measurements on patients. In such cases, we can use a similar approach after the implementation of initial constraints e.g., from ECG.

Acknowledgements

Data for this study were obtained from the EDGAR database and provided by the CVRT and CSI Institute at the University of Utah, by the IHU-LIRYC Institute at the Université de Bordeaux and by the Institute of Measurement Science, SAS in cooperation with the National Institute for Cardiovascular Diseases, Bratislava, Slovakia. This work was supported by the research grant 2/0125/19 from the VEGA Grant Agency in Slovakia and by the grant APVV-19-0531 from the Slovak Research and Development Agency.

References

- [1] L.R. Bear et al., "Advantages and pitfalls of noninvasive electrocardiographic imaging," *J. Electrocardiol.*, vol. 57, no. Suppl., pp. S15-S20, Nov.–Dec. 2019.
- [2] S. Yamashita et al., "High-density contact and noninvasive mapping of focal atrial tachycardia: Evidence of dual endocardial exits from an epicardial focus," *Pacing Clin Electrophysiol*, vol. 41, no. 6, pp. 666–668, Jun 2018.
- [3] J. Svehlikova et al., "Geometrical constraint of sources in noninvasive localization of premature ventricular contractions," *J. Electrocardiol.*, vol. 51, no. 3, pp. 370–377, May-June 2018.
- [4] F. Gharbalchi et al., "Reduced leadset selection and performance evaluation in the inverse problem of electrocardiography for reconstructing the ventricularly paced electrograms," *J. Electrocardiol.*, vol. 60, pp. 44–53, May-June 2020.
- [5] L. Parreira et al., "Electrocardiographic imaging (ECGI): What is the minimal number of leads needed to obtain a good spatial resolution?," *J. Electrocardiol.*, vol. 62, pp. 86–93, Sep. – Oct. 2020.
- [6] K. Aras et al., "Experimental data and geometric analysis repository - Edgar," *J. Electrocardiol.*, vol. 48, no. 6, pp. 975-981, Nov-Dec. 2015.
- [7] B. Ondrusova et al., "Significance of multi-lead ECG electrodes derived from patient-specific transfer matrix", *2021 13th International Conference on Measurement*, pp. 80-83, May 2021.

Address for correspondence:

Beata Ondrusova
Institute of Measurement Science, Slovak Academy of Sciences
Dubravská cesta 9, 84 104 Bratislava, Slovakia
umerondb@savba.sk